Synthesis and Degradation of Agar-Carbomer Based Hydrogels for Tissue Engineering Applications

Filippo Rossi,[1,2] Xanthippi Chatzistavrou,[2] Giuseppe Perale,[1] Aldo R. Boccaccini[2,3]

[1]*Department of Chemistry, Materials and Chemical Engineering "Giulio Natta", Politecnico di Milano, Via Mancinelli 7, 20131 Milano, Italy*
[2]*Department of Materials, Imperial College London, Prince Consort Rd., London SW7 2BP, UK*
[3]*Institute of Biomaterials, Department of Materials Science and Engineering, University of Erlangen-Nuremberg, 91058 Erlangen, Germany*

Received 11 November 2010; accepted 11 March 2011
DOI 10.1002/app.34488
Published online 27 July 2011 in Wiley Online Library (wileyonlinelibrary.com).

ABSTRACT: Hydrogels studied in this investigation, synthesized starting from agarose and Carbomer 974P, were chosen for their potential use in tissue engineering. The strong ability of hydrogels to mimic living tissues should be complemented with optimized degradation time profiles: a critical property for biomaterials but essential for the integration with target tissue. In this study, chosen hydrogels were characterized both from a rheological and a structural point of view before studying the chemistry of their degradation, which was performed by several analysis: infrared bond response [Fourier transform infrared (FT-IR)], calorimetry [differential scanning Calorimetry (DSC)], and % mass loss. Degradation behaviors of Agar-Carbomer hydrogels with different degrees of crosslinkers were evaluated monitoring peak shifts and thermal property changes. It was found that the amount of crosslinks heavily affect the time and the magnitude related to the process. The results indicate that the degradation rates of Agar-Carbomer hydrogels can be controlled and tuned to adapt the hydrogel degradation kinetics for different cell housing and drug delivery applications. © 2011 Wiley Periodicals, Inc. J Appl Polym Sci 123: 398–408, 2012

Key words: hydrogels; degradation; FT-IR; scaffold; tissue engineering

INTRODUCTION

Tissue or organ transplantation is severely limited by the problems of donor shortage and immune rejection from receiving patients. Developments and recent achievements on tissue engineering allow the transplantation of cells from a patient's own tissue to regenerate damaged tissues or organs, avoiding adverse immune responses.[1,2] Several recent researches point towards the combined use of cells together with specific drugs to enhance regenerative therapeutic effects.[3,4] In this framework, three-dimensional (3D) biomaterial-made scaffolds were first developed as a temporary substrate to grow cells in an organized fashion, before performing the transplantation of such combined structures.[5] Direct injection of *in vitro* cultured cells is one attractive alternative,[6] but it sees deep concerns emerging as trials are performed: injected cells very often leave the zone of injection, as they are not confined by any support, and easily get into the circulatory torrent migrating all over the body towards a rather uncertain fate. Thus, not only scientific literature but also regulatory supranational directives (e.g., EU668/2009 and 47/2007/EC) are now pointing towards the combined approach of cells and adequate support structures, specifically to avoid migration of cells outside the target area. As a result, strong attention on polymers is confirmed as they can be used not only to fabricate 3D scaffolds but also to develop injectable systems for tissue engineering.[6–11] Indeed, in the wide field of biomaterials, one of most suitable classes for these purposes is surely represented by hydrogels.[5,6,9,12,13] They can be designed as temporary structures having desired geometry and physical, chemical, and mechanical properties adequate for implantation into chosen target tissue. Nevertheless, care must be taken not only to ensure complete biocompatibility of both intermediate and final degradation products but also to provide a degradation kinetic compatible with host tissue integration, to allow proper and viable tissue regenerative processes.[14–16] Here, where drugs and cells are loaded for local delivery purposes, attention must be paid to hydrogel chemical structure because a premature degradation might lead to excessively fast drug release and to cell escape earlier than adequate tissue formation; on the other hand, a delayed degradation may result in insufficient nutrient transport and/or physical space that impede formation of a fully competent tissue, together with a too slow drug delivery.[14,17,18]

Correspondence to: G. Perale (giuseppe.perale@polimi.it).

In this framework, this work regards a particular kind of hydrogels (here briefly indicated with the *AC* acronym) synthesized by copolymerization between two polymers: the first being agarose, a commonly used natural polysaccharide,[18] whereas the second being Carbomer 974P,[19] a highly branched synthetic polyacrylic acid commonly used in biomedical and pharmaceutical applications. Previous investigations suggested that by tuning crosslinkers concentrations obtained hydrogels can be either promising scaffolds for cell housing, particularly for cells of the central nervous system (CNS) and stem cells,[20,21] or suitable carriers for pharmacological treatments.[22] Moreover *in vivo* investigations confirmed very high biocompatibility. These preliminary studies also allowed to state that *AC* hydrogels can be injected into spinal cord parenchyma for local therapies achieving *in situ* gelation that is an essential feature for regenerative medicine.[23]

The aim of the present work was to study the degradation of *AC* hydrogels and its fine control[24,25]: it was monitored via Fourier transform infrared (FT-IR) spectroscopy measurements, by differential scanning calorimetry (DSC) analysis, and % mass loss.[24,26,27] Moreover, the hydrogel inner morphology and its nanometric nature were investigated by transmission electron microscopy (TEM). As described,[20] *AC* gels can be considered a "material library," and thus, investigations were here performed only on *AC1* and *AC6* samples, because they represent the two limits, lower and upper, respectively, of the explored crosslinkers ratios range.

MATERIALS AND METHODS

Materials

Materials used for hydrogel preparation were the following: Carbomer 974P (CAS 151687-96-6, Fagron, The Netherlands), triethyl-ammine (*alias* TEA, CAS 121-44-8, high purity preparation by Sigma-Aldrich, Germany), propylene glycol (CAS 504-63-2, by Sigma-Aldrich, Germany), glycerol (CAS 56-81-5, by Merck Chemicals, Germany), and agarose (CAS 9012-36-4, by Invitrogen Corp., Carlsbad, CA).[20] The solvent used was Dulbecco's Phosphate-Buffered Saline (pH = 7.4) solution (*alias* PBS, Sigma-Aldrich, Germany) which allowed us to keep gelation under strict control.[20] All materials were used as received.

Hydrogel synthesis

Hydrogels were synthesized by bulk reaction in PBS, at about 80°C. Polymeric solution was achieved by mixing polymer powders in the solvent, adding a mixture of crosslinking agents made of propylene glycol and glycerol along with TEA. The reaction pH was kept neutral. The onset of gelation was achieved by means of electromagnetic (EM) stimulation. Indeed, these groups constitute the crosslinking sites, particularly those of propylene glycol and glycerol, to be reacted with those of Carbomer and agarose, altogether giving rise to the 3D matrix. Effective gelation and reticulation were achieved applying EM (500 W irradiated power) heating in ratio of 1 min per 10 mL of polymeric solution.[20] Gelation was achieved during cooling down to room temperature in a 48-multiwell cell culture plate (Corning Costar, Corning, NY). As said, only *AC1* and *AC6* gels were investigated; the composition in terms of weight for *AC1* are: 98.52% PBS, 0.49% Carbomer 974P, 0.49% agarose, and 0.5% TEA; whereas for *AC6* are: 67% PBS, 0.49% Carbomer 974P, 0.49% agarose, 30.3% propylene glycol, 1.22% glycerol, and 0.5% TEA. The difference between the two formulations investigated regards crosslinkers, present only in *AC6* formulation, which affects not only the chemistry of polycondensation but also the macroscopic characteristics. Acronyms of hydrogels (i.e., *AC1*, *AC6*) are harmonized with previous studies where differences in terms of physical properties (mesh size, average molecular weight between two following crosslinks, and crosslinking density) and rheological behavior were analyzed. The interest in, at least two different formulations, is due to their different characteristics which make the first one (*AC1*) more suitable in low viscosity applications, e.g., in controlled drug delivery applications (i.e., 6–48 h),[22] whereas the second one (*AC6*) is more adequate for hosting cells for longer time frames (i.e., 4–5 weeks) as CNS applications might require.[21,22]

Swelling behavior and degradation

The hydrogel samples were first immersed in PBS for about 24 h, then freeze-dried, weighted (W_d), and poured in excess PBS or DMEM (Dulbecco's modified eagles medium) to achieve complete swelling at 37°C in 5% CO_2 atmosphere; such conditions were considered because typical of *in vitro* experiments. The swelling kinetics was measured gravimetrically. The samples were removed from the solvent at regular times. Then, hydrogel surfaces were wiped with moistened filter paper to remove the excess of solvent and then weighed (W_t). Swelling ratio is defined as follows:

$$swelling\ ratio = \frac{W_t}{W_d} \cdot 100 \quad (1)$$

where W_t is the weight of the wet hydrogel as a function of time and W_d of the dry one. Degradation of hydrogels was also examined with respect to

weight loss. Weight loss of initially weighed hydrogels (W_0) was monitored as a function of incubation time in PBS at 37°C in 5% CO_2 atmosphere. At specified time intervals, hydrogels were removed from the PBS and weighed (W_t). The weight loss ratio was defined as: $100\% \times (W_0 - W_t)/W_0$.

Mesh size: Flory–Rehner theory

According to the Flory–Rehner equation, swelling data can be used to evaluate some important structural parameters of the hydrogel such as: (a) the average molecular weight of the chain between two following crosslinks, M_c (g/mol), (b) the crosslinkage density ν (mol/cm^3), expressed by the ratio between the number of moles between two following crosslinks and the volume of dry polymer, and (c) the mesh size ζ (nm), defined as the length of the polymer chain between two following crosslinks.[12,28] When a polymer network is swollen, its chains achieve elongated conformation; such elongation is contrasted by an opposite elastic force, thus limiting the chain stretching. On the other hand, the polymer–solvent mixing increases the system entropy, thus favoring the hydrogel swelling towards lower free energy configurations. At equilibrium, such opposite forces are balanced, and the maximum swelling extent is achieved.

Using a simplified version of the Flory–Rehner equation,[12,28] the average molecular weight M_C was evaluated as a function of the volumetric swelling ratio, Q_V as:

$$Q_V^{5/3} = \frac{V_p \cdot M_C}{V_1} \cdot (0.5 - \chi) \tag{2}$$

In this equation, V_p is the specific volume of dry polymer, V_1 the specific volume of the solvent (PBS), and χ the Flory interaction parameter between polymer and solvent.[29,30] Q_V was evaluated from the mass swelling ratio (Q_M) through the following equation:

$$Q_V = 1 + \frac{\rho_p}{\rho_s} \cdot (Q_M - 1) \tag{3}$$

where ρ_p is the density of the dry polymer and ρ_s that of the solvent.

The crosslinkage density was determined as[31]:

$$\nu = \frac{\rho_p}{M_C} \tag{4}$$

and the swollen hydrogel mesh size was calculated using the following equation[32]:

$$\zeta = Q_V^{1/3} \cdot \sqrt{r_0^2} \tag{5}$$

where $\sqrt{r_0^2}$ is the root main square distance between crosslinks.

Rheological properties

Rheological analysis was performed at 37°C using a Rheometric Scientific ARES instrumentation (TA Instruments, New Castle, DE, US) equipped with 30 mm parallel plates, with a 4 mm gap between them. Typical body temperature was selected to be consistent with the biomedical application. Oscillatory responses (G', elastic modulus and G'', loss/viscous modulus) were determined at low values of strain (0.02%) over the frequency range 0.1–100 rad/s.

Transmission electron microscopy

TEM experiments were performed using a CM200 microscope (Philips BV, The Netherlands) at 200 kV accelerating voltage. Samples were immersed in a 20-fold solution of pure ethanol, as a very volatile solvent, and stirred vigorously.[25] A 5 μL drop of the resulting suspension was then applied onto a carbon coated polyvinyl formal (Formvar) grid. Grid was blotted after 60 s and left to air dry. A 5 μL drop of 2% (wt/vol) uranyl acetate (Agar Scientific, UK) water solution was subsequently placed on the grid, blotted after 30 s, and air dried. The obtained samples were then examined by TEM.[17,25,33] Moreover, to observe the network structure without the presence of vitrified ice within the *AC* matrix, water was allowed to sublimate (at pressure corresponding to the vacuum of the TEM column) by *in situ* freeze-drying of the samples.[34,35]

Analytical methods

Fourier transform infrared spectroscopy

Hydrogel samples were immersed for 24 h in excess of PBS. Samples were then freeze-dried and laminated directly with potassium bromide.[36] Infrared spectra were then recorded using the TENSOR Series FT-IR Spectrometer (Bruker, Germany). For each sample, scans were recorded between 4000 and 500 cm^{-1}.

Experiment 1.. Hydrogel samples were first freeze-dried for about 24 h, then immersed in excess of PBS to swell, and then degrade, being kept at 37°C in a 5% CO_2 atmosphere typical of biological *in vitro* experiment. Samples were removed from PBS (after 1, 2, 3, 7, 14, and 28 days) and compared with dry samples, i.e., those that were freeze-dried but not immersed in PBS. All these samples were analyzed using FT-IR instrument collecting the transmittance signal.

Experiment 2.. Hydrogel samples were synthesized and then immediately immersed in excess of PBS, being kept at 37°C in a 5% CO_2 atmosphere, thus allowing swelling kinetic and degradation by hydrolysis to occur immediately after synthesis. They were then extracted (after 1, 2, and 4 weeks) and freeze-dried for 24 h. In the end, they were analyzed using same FT-IR instrument collecting the transmittance signal.

DSC

Hydrogel samples were synthesized and then immediately immersed in excess of PBS, being kept at 37°C in a 5% CO_2 atmosphere, thus allowing swelling kinetic and degradation to occur immediately after synthesis. They were then extracted (immediately and after 4 weeks) and freeze-dried for 24 h before undergoing thermal analysis which was performed in a Perkin–Elmer DSC (Pyris software 3.81): samples were heated from 25 to 1000°C at a heating rate of 10°C/min.

Statistical analysis

Data were analyzed using *t*-test for differences. Results are reported as mean ± standard deviation. The significant level was set as $P < 0.05$.[17]

RESULTS AND DISCUSSION

Hydrogel synthesis and characterization

Hydrogels here investigated were synthesized starting from a branched polyacrylic acid (Carbomer 974P) and agarose, a common polysaccharide. The condensation reaction was microwave assisted to obtain a chemically crosslinked hydrogel, as verified with FT-IR analysis.[20] Within the unirradiated solution, polymer chains are not overlapped, and thus, segmental mobility is high. At low irradiation doses, intramolecular links and chain scissions are favored. The decrease, in segmental mobility, allows intermolecular crosslinks to be formed and thus giving origin to local 3D networks, also known as "microgels." Increasing irradiation, intermolecular crosslinking, and chain scission are massively privileged, thus giving origin to macroscopic gels.[28] Nevertheless, crosslinked gels are not truly homogeneous because clusters of molecular entanglements, hydrophobically domains, or ionically-associated ones can create local heterogeneities. Chemical interactions would statistically bring polymer chains together and, indeed, the formation of a stable structure occurs through junction zones between chains (as simplified by Scheme 1). The presence of hydroxyl groups (hereinafter indicated by letter *A*, present in agarose, glycerol, and propylene glycol) and carboxyl ones (hereinafter indicated by *B*, present in Carbomer 974P) suggests that main interactions occur via esterification and hydrogen bonding (chemical hydrogel), as confirmed by FT-IR analysis. The esterification takes place between Carbomer 974P and either agarose or glycerol or propylene glycol. Moreover, PBS salts freely solvated in water cause salt carboxylates formation. Due to these reactions, *AC* hydrogels are quite anionic and this electrostatic nature, confirmed by mass equilibrium swelling at different pH,[20] influences the ability and the kinetics involved in drug delivery.[22] Theoretical generic structure of *AC* hydrogel, considered as an ideal network, is sketched in Scheme 1. This idealized structure allows understanding and rationalizing of degradation mechanisms.

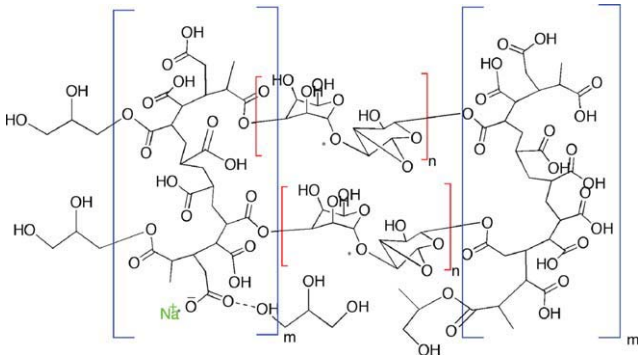

Scheme 1 Scheme of the three-dimensional network formed by statistical polycondensation between Carbomer 974P (blue), agarose (red), and crosslinking agents in phosphate buffer saline solution (green). Esterification, hydrogen bonding and carboxylation bring statistically closer the polymer chains, thus creating a stable heterogeneous structure. [Color figure can be viewed in the online issue, which is available at wileyonlinelibrary.com.]

ATR spectra of the compared physical and chemical hydrogels, i.e., before and after microwave irradiation, were already presented in previous study[20]: the differences between the two spectra were in peaks corresponding to symmetric (1406 cm^{-1}) and asymmetric CO_2 stretches (1560 cm^{-1}), due to the esterification.

AC hydrogels can be rightfully considered a "material library" where dissimilarities lie in different amount of crosslinkers involved in polycondensation, identified, and briefly described through the ratio between hydroxyl and carboxyl groups (*A*/*B*). Accordingly, *AC6* presents a higher *A*/*B* ratio, which affects not only its microchemistry but also its physical properties. The swelling kinetics of the hydrogel studied in PBS, kept at 37°C and 5% CO_2 atmosphere, are presented in Figure 1 (typical controlled environment used for *in vitro* biological experiments). All samples exhibited fast swelling kinetics,

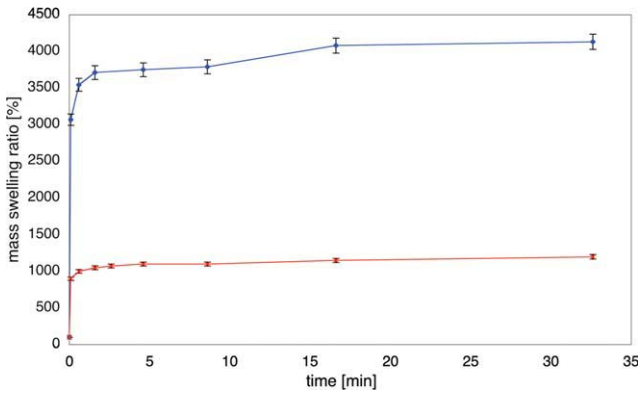

Figure 1 Swelling behavior of *AC* hydrogels in phosphate buffer solution at 37°C and 5% CO_2 atmosphere: the less crosslinked hydrogel *AC1* (blue) exhibits a higher ability to retain water within it with respect to the highly crosslinked *AC6* (red). [Color figure can be viewed in the online issue, which is available at wileyonlinelibrary.com.]

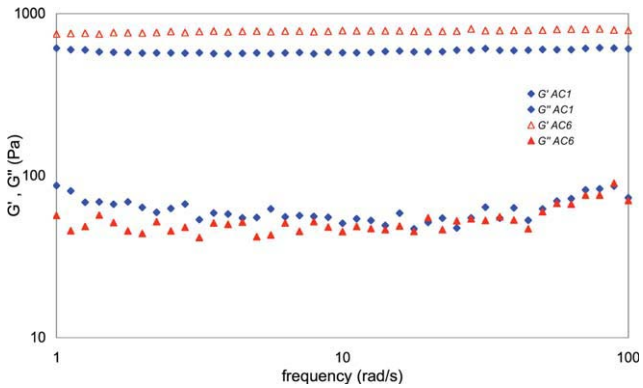

Figure 2 Mechanical spectra of *AC1* (in blue) and *AC6* (in red) gels at room temperature with small oscillatory shear in the linear viscoelastic regime: G' and G'' are frequency independent, indicating dominant viscoelastic relaxations at lower frequencies. [Color figure can be viewed in the online issue, which is available at wileyonlinelibrary.com.]

and they reached swelling equilibrium within the first hour.

Compared with the hydrogel with larger amounts of reacting groups (*AC6*), hydrogels with smaller amounts of *A* groups (*AC1*) displayed higher swelling ratio at equilibrium. The differences, experimentally observed, can be attributed to a higher ability to retain water when the amount of crosslinkers is smaller. Indeed, increasing *A*/*B* ratio, water molecules cannot easily diffuse into the hydrogel network, leading to a reduced volumetric expansion and therefore resulting in a denser network.

Figure 2 shows a Dynamic Frequency Sweep test (DFS) spectra performed at 37°C for both gels. In both cases, storage modulus (G') is found to be approximately one order of magnitude higher than the loss modulus (G''), indicating an elastic rather than viscous material. Furthermore, both G' and G'' of each gel are essentially independent from frequency over the entire investigated range, thus indicating dominant viscoelastic relaxations of networks at lower frequencies. This means that network relaxation time, τ, is rather long ($\tau \approx 2000$ s). Such rheological behavior matches the characteristic signature of a solid-like gel, confirming this nature for both *AC* type gels. The values obtained for G' ($\sim$ 600 Pa for *AC1* and $\sim$ 750 Pa for *AC6*) are of the same order of magnitude as the modulus reported in the literature for other biopolymers and hydrogels.[25] As expected, *AC6* behaves as a more rigid network than *AC1*, and this is in perfect agreement with structural differences due to the presence of crosslinkers, as also shown by swelling studies.

Complete FT-IR spectra of raw polymers and both *AC1* and *AC6* gels are plotted in Figure 3. Both spectra show a broad peak around 3450 cm^{-1}, which is due to the stretching vibration of O—H bonds, whereas peaks around 2940 cm^{-1} are due to the C—H stretch. According with our hypothesis, the formation of ester bonds is visible in peaks corresponding to symmetric (around 1600 cm^{-1}) and asymmetric (around 1400 cm^{-1}) CO_2 stretches. Moreover, the presence of TEA inside the network, related to C—N vibration, is confirmed by the peaks around 1080 cm^{-1}. Spectra also show, in the range 900–1000 cm^{-1}, peaks related to C—O—C stretch vibration that represents the glycosidic bond

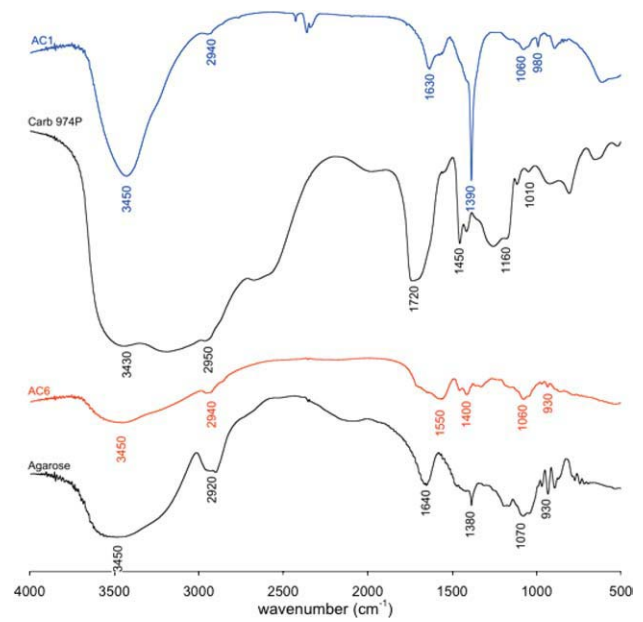

Figure 3 Fourier transform infrared (FT-IR) spectra for both *AC1* (blue plot) and *AC6* (red plot) gels plotted versus spectra of polymers involved in the reaction (Carbomer 974P and agarose, both in black plots): hydrogels share analogies and show some differences compared with bare polymers. [Color figure can be viewed in the online issue, which is available at wileyonlinelibrary.com.]

TABLE I
Hydrogel Physical Characteristics Estimated Through the Flory–Rehner Theory (s.d. ± 2.5%)

Samples	ζ (nm)	M_c (g/mol)	ν (mol/cm^3)
AC1	90	15,540	113
AC6	28	3450	506

between monosaccharides (typical of agarose structure) and ester groups.

The building blocks, or subunits, of macromolecules form a stable structure made up mostly of C—C bonds, usually referred as the "carbon skeleton." C—C and C—H bonds are said to be nonpolar and thus tend to be lowly reactive and sometimes behave inertly at our degradation conditions. Building blocks of macromolecules act as discrete subunits because their internal structure consists of C—C bonds; the links between the subunits are made by C—O and/or C—N bonds: indeed, degradable bonds generally involve oxygen or nitrogen atoms. Here, the obtained FT-IR results allow stating that the most important groups in the studied gels are: —OH, C—H, CO_2 (i.e., carboxylates), vinyl, C—N, and C—O—C.

The chemical characterization of hydrogels is well known for being a difficult task; this is mainly due to the casual chemical rearrangement of the network structure and the random crosslinks occurring during gelation.[37] In Table I, the estimated values of the mesh size (ζ), average molecular weight between two following crosslinks (M_c), and crosslinking density (ν) are summarized. The effect of the crosslinkers (increasing from *AC1* to *AC6*) was to make more compact the hydrogel structure: as a matter of fact, estimated mesh sizes decreased from 90 nm (*AC1*) to 28 nm (*AC6*). Moreover, if we consider an increase in mesh size, corresponding decrease in crosslinking density and increase in molecular weight M_c are found. This is reasonable because, in hydrogels with higher mesh size values, two following crosslinks are farther from each other: therefore, the molecular weight between two following crosslinks is higher and crosslinking density lower. With reference to the values of A/B ratio, it is now useful to re-examine how crosslinking agents influence physical characteristics. Due to the bonds between the hydrophilic groups, the whole gel network is more compact, and less water is absorbed when hydroxyl groups prevail on carboxyl ones ($A/B \gg 1$): mesh sizes decrease as the ratio increases. Lower ability to retain water corresponds to lower mesh size and average molecular weight values.

These studies were completed by direct observation of the gel 3D network by means of TEM imaging. This allowed investigation on how polymers arranged themselves during the gelation process: imaging was performed immediately after gelation, thus providing both information on state of the hydrogel before degradation ($t = 0$) and a detailed snapshot of the local morphology at the nanoscale. It is worth to point out here that the importance for biomaterials of being "nanostructured" is widely discussed in the literature[38,39]: cells are in the scale of microns, but extracellular matrices (ECMs) have intimate structures in the nanoscale ,and biomaterials for cell housing shall indeed mime the various kind of ECMs. The use of TEM imaging allowed us to analyze dried samples which have the same 3D polymeric configuration of wet ones[25]: the experimental result in terms of average mesh size appeared directly comparable with theoretically calculated one.

From image (a) in Figure 4, a chaotic and not regular state of matter is evident in an *AC1* sample: this structure is typical of solid-like gels.[25,28]

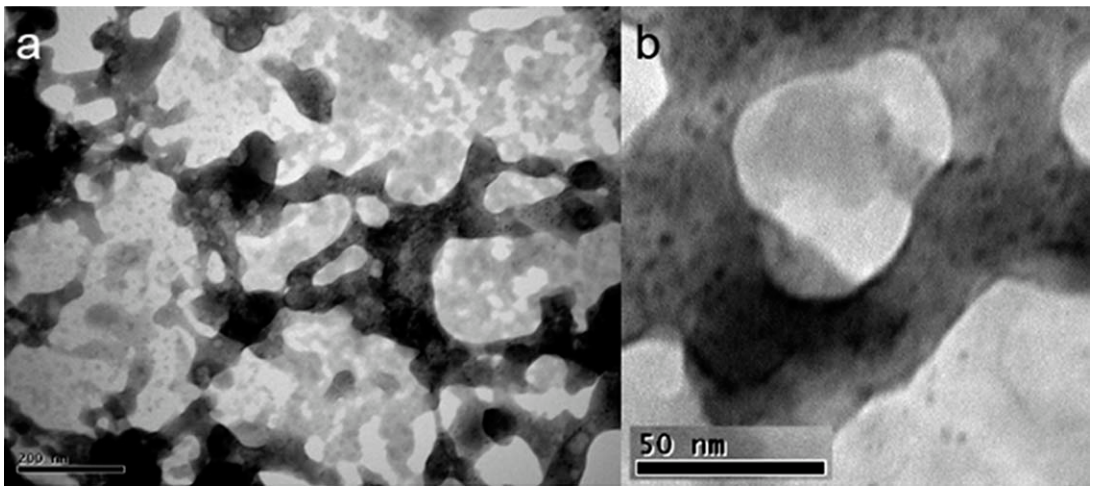

Figure 4 Transmission electron micrographs of hydrogel AC1 at two magnifications, where the scale represents: (a) 200 nm and (b) 50 nm.

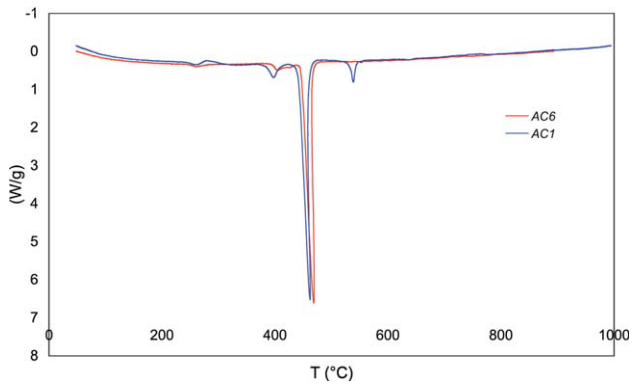

Figure 5 DSC thermograms of gel samples *AC1* (blue) and *AC6* (red), both taken immediately after gelation (t_0). [Color figure can be viewed in the online issue, which is available at wileyonlinelibrary.com.]

Nevertheless, if gelation is properly controlled, Flory–Rehner theories provide powerful tools to describe hydrogel structure by means of mean values per volume unit: mean mesh size being one of the most relevant and meaningful parameters. The mean mesh size resulted about 90 nm. Micrograph in Figure 4(b) shows the detail of a mesh in an *AC1* sample, having diameter in the range of 100nm. This mean value is respected in all the micrographs collected along other different focal planes. Here, for sake of clarity, only a global overview and a particular mesh are presented [Fig. 4(a,b)].

Coherently with *AC1* data, including rheological data presented above and from previous studies, *AC6* samples were expected to be, and indeed were, much tighter than *AC1* samples, and *AC6* samples should exhibit much smaller mesh size, of about 25 nm in average. This indication was indirectly confirmed by TEM as technical sample manipulation limits did not allow achieving a clear image of *AC6* meshes.

Thermal properties were obtained through DSC analysis and are presented in Figure 5, where the differences between the two hydrogels are underlined: glass transition temperature (T_g) of the synthesized hydrogels increases, from 237 to 245°C, with the increasing of A/B ratio, indicating that chain flexibility decreases. This is due to the higher presence of crosslinks that involves the formation of intermolecular connections through chemical bonds that necessarily results in a reduction of chain mobility and of the free volume. Figure 5 also shows a very visible peak at around 400°C: it corresponds to the oxidative degradation: 462°C for *AC1* and 469°C for *AC6.* In general, above T_g the mobility of the polymeric network increases, and residual acrylic acid monomer is released. Then, thermal degradation (from 400°C) is characterized by the complete mass loss which is largely due to oxydative degradation in terms of depolymerization. It starts with the shortest polymer chains (400°C for *AC1* and 408°C for *AC6*) and subsequently, following this increasing trend with the others, with the average-long polymer chains value (462°C for *AC1* and 469°C for *AC6*). The residual mass loss thus corresponds to the longest chains that are degradated at 539°C for *AC1* and 550°C for *AC6*.[40,41] This peak values increase as crosslinking density increases, indicating that thermal stability increases with mechanical and physical properties of the 3D network. Thus, the smaller the mesh size, the higher the material stability.

Hydrogel degradation

As discussed above, the study of statistical polycondensation allows to simplify the polymeric network of *AC* gels as a C—C backbone, from Carbomer 974P, esterified with agarose, propylene glycol, glycerol, and salt present in PBS. During the hydrolysis reaction, esters become carboxylic acid with the consequent crosslinking loss, following the proposed reaction:

$$RCO_2R' + H_2\,O \rightarrow RCO_2H + R'OH$$

Spectra for *AC1* gel before and during hydrolytic degradation are presented in Figure 6.

Starting from the dry sample (day 0), the following aspects can be observed: —OH peak stretch (3247 cm^{-1}), asymmetric C—H stretch (2943 cm^{-1}), asymmetric CO_2 stretch (1638 cm^{-1}), symmetric CO_2 stretch (1385 cm^{-1}), asymmetric C—O—C (1080 cm^{-1}), C—N bend (1042 cm^{-1}), vinyl group (990 cm^{-1}), and symmetric C—O—C stretch (892 cm^{-1}). Considerable information can be drawn from these plots. First, the —OH peak stretch is common in this type of materials because of the large amount of hydroxyl groups present and, as the hydrolysis starts, its contribution increases, and the area thus becomes larger and rounded. From the plot, it is visible that, increasing the time of exposure to PBS, the —OH peak in the polymer becomes similar to the —OH peak present in a classic FT-IR water spectrum. Secondly, the C—H stretch peak (2943 cm^{-1}) shows that the C—H bond is not easily degradable because of its low polarity. Nevertheless, its shape apparently changes during degradation, but the peak maximum remains at the same wave number value thus confirming that it is not affected by degradation. This peak shape is different because the proximity with the —OH region seems to cover it, in fact this peak is not visible in a wet sample. Third, it is also possible to observe a region between 2250 and 2000 cm^{-1} where both present peaks and their area increase during degradation. This wave number region is typically present in water spectrum and it

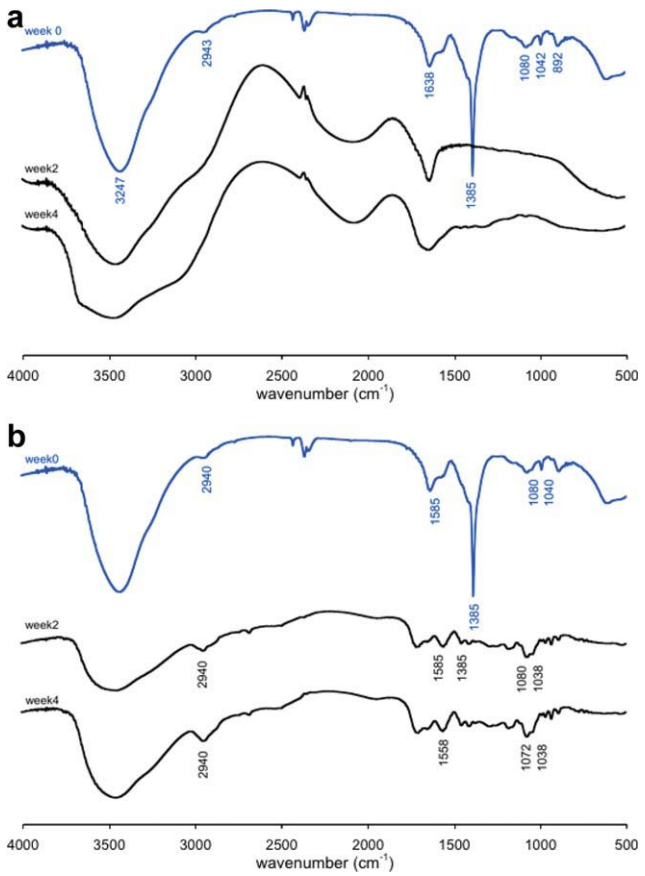

Figure 6 (a) FT-IR spectra of *AC1* (blue) before and after 2 and 4 weeks of degradation in PBS (black). (b) FT-IR spectra of dried *AC1* hydrogel (blue line) before and after 2 and 4 weeks of degradation in PBS (black plots). Peak shift describes the degradation of the three-dimensional network. The absence of water allows a better resolution and rationalization: particularly the —OH stretch increases its area due to ester bonds hydrolysis. [Color figure can be viewed in the online issue, which is available at wileyonlinelibrary.com.]

presence, increasing during time, means that the macromer concentration decreased. Next to this last region, there are two peaks corresponding to CO_2 (carboxylates) stretches. Fourth, one of most important peak in water spectrum is around 1600 cm^{-1}. As hydrogel degradation proceeds, this peak becomes more evident, and it progressively covers the asymmetric CO_2 stretch. Peak maximum, as degradation proceeds, moves toward lower wave numbers, more pronouncedly in hydrogels with short chains, which confirms their faster degradation due to lower hydrophobicity. This behavior indicates a reduction in bonds number within the hydrogel, being due to degradation. Fifth, the two peaks reflecting C—O—C stretch and C—N bonds show the same trend, with decreasing peak maximum, thus meaning that they are being hydrolyzed. Sixth, other well detectable peaks correspond to vinyl group and symmetric C—O—C stretch; this last is obscured by water contribution signal. On the other hand, the vinyl group disappears rapidly because its hydratation is thermodynamically enhanced, and its product is an alcohol, which contributes to increase the —OH stretch peak area, as expected.

It is evident that degradation takes place mostly between the first and the second week, widely in agreement with mean medical requests for a resorbable hydrogel for tissue engineering. It could allow a complete and efficient drug delivery capability, maintaining also adequate mechanical properties for tissue scaffolding functions.[14]

The presence of water produces a strong and wide IR signal, covering significant information. It is therefore necessary to carry out experiments on dry samples, to extract more detailed information (Experiment 2). Relevant *AC1* spectra taken on dried samples before and during degradation are presented in Figure 6(b).

Spectra achieved during this second experiment showed the presence of all meaningful peaks during the whole degradation process, from day 0 through all time points. This data enable a better hydrolysis rationalization and a more detailed understanding of all phenomena involved. However, also in absence of water, the first —OH stretch peak (around 3400 cm^{-1}) increases its area from time to time following the ester hydrolysis trend: as explained above the products are carboxylic acids and alcohols.

From spectra reported in Figure 6(b) ,the presence of a substantial amount of carboxylates can be observed. This bond type is well hydrolysable because of the high electronegative difference between the carbon and oxygen atoms involved. Indeed, during time, the two peaks expression of ester hydrolysis, i.e., C=O (1700 cm^{-1}) and C—O (1310 cm^{-1}) stretches of carboxylic acids, become visible.

As degradation proceeds, peaks maxima move toward lower wave numbers, an effect that is very pronounced in hydrogels with short chains, confirming their faster degradation due to their lower hydrophobicity. Similarly, the two peaks reflecting C—O—C stretch and C—N bonds show the same trend, with decreasing peak maximum meaning they are being hydrolyzed during degradation. The first one is extremely important as it indicates the polysaccharidic fraction hydrolysis that occurs through ester bond cleavage.

It can be immediately noted that C—H stretches show a constant trend during time, which reflects the bond apolar nature. Oppositely, other stretches and bonds show different but decreasing trends, each one reflecting the differences of their hydrolizability. From these data, it is also evident that degradation plays a key role between the first and second weeks, being an indication of suitable behavior for

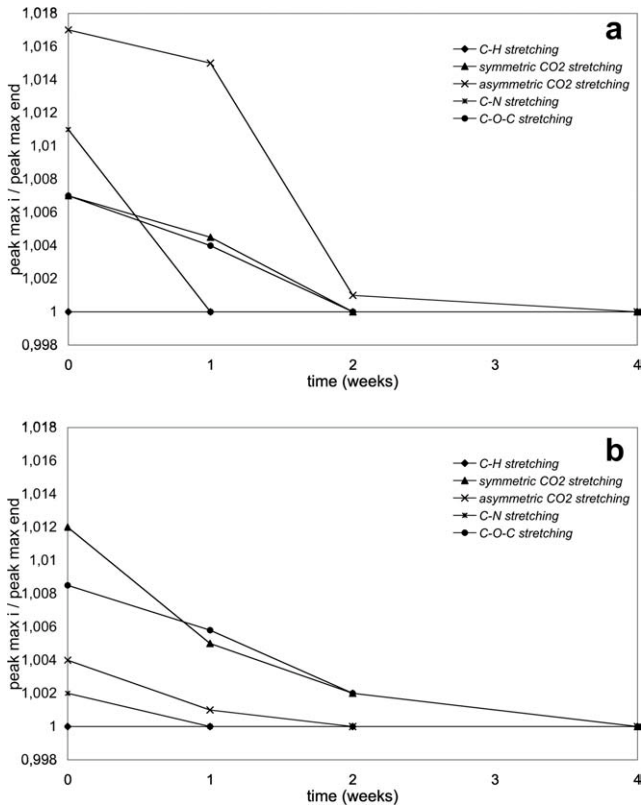

Figure 7 (a) Trend of stretching peaks shift (relative percentage) during degradation for *AC1* hydrogels. The degradation plays a key role between the first and the second week. (b) Peaks shifts during *AC6* hydrolysis: C—H remains constant due to its apolarity, CO_2 decreases because of ester hydrolysis and C—O—C degrades through glycosidic bond cleavage.

drug delivery applications. In particular, carboxylates are decreasing for the reasons discussed above, and at the same time also the C—O—C stretch is decreasing.

Moreover, always considering *AC1* samples, results of DSC measurements conducted both before and after 4 weeks of degradation in PBS, are assessed. The key parameter studied is T_g, glass transition temperature, which reflects chain mobility and consequently networks arrangement. Changes on T_g of both *AC1* and *AC6* samples during degradation are presented in Figure 5. It is evident that during hydrolysis T_g decreases from 237 to 234°C. The decrease in T_g values on degradation might be due to the loss of ester units via hydrolysis and, correspondingly, to the increase of pure polymer fraction of the 3D network with a consequent increase of chain mobility and free volume.[26,42]

Effect of crosslinks on hydrogel degradation

Relative peak shift values for *AC6* degradation (Experiment 2) are presented in Figure 7(b). At a first glance, it can be noted that all patterns are comparable with those of *AC1* gels, reported in Figure 7(a).

Nevertheless, it has to be underlined that the time scale of degradation is similar for both gels but, when considered in deeper details, *AC6* hydrogels, being a more compactly crosslinked gel, degrade slower than *AC1* samples. Indeed, it has to be precisely observed that *AC6* starts to degrade during first week, similarly to *AC1*, but then the following trend is much slower with respect to *AC1*. This behavior is justifiable because, as degradation occurs, the hydrolytically labile bonds in the network are cleaved throughout the entire hydrogel at a rate controlled by the reaction kinetics for their hydrolysis. This ongoing cleavage of labile bonds within the hydrogel systematically decreases the crosslinking density of the overall structure. Moreover, the higher and quicker ester hydrolysis in *AC1* is also due to the lower viscosity of the polymeric network, compared with *AC6* where the high amount of propylene glycol and glycerol influence its value. The lower viscosity indeed allows higher chain mobility and diffusion and, consequently, a faster degradation. Following the degradation of those bonds, the *AC6* gel structure will degrade too, but it will still be more compact during time with respect to *AC1* gel that was shown to have a much lower crosslinks density (lower A/B). Consequently, *AC6* could be useful for different *longer time* applications in medicine than *AC1*.[43] Degradation of hydrogels was monitored also as a function of weight loss during incubation time in PBS at 37°C, as shown in Figure 8. The ratio of crosslinkers had a significant influence on weight loss. The hydrogels with a lower ratio showed a significantly faster weight losing rate due to less

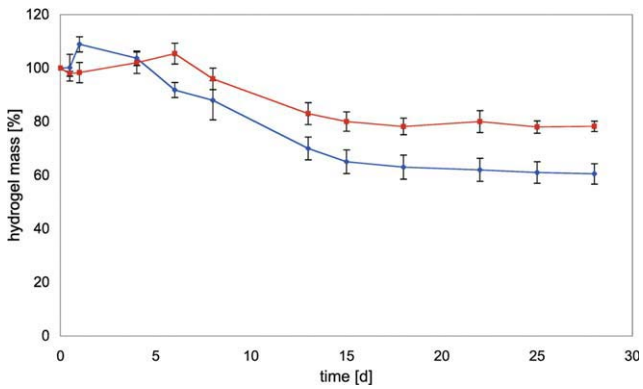

Figure 8 Degradation of *AC1* (blue) and *AC6* (red) hydrogels in PBS at 37°C with respect to weight loss. [Color figure can be viewed in the online issue, which is available at wileyonlinelibrary.com.]

crosslinking. They lost their weight steadily up to 28 days (Fig. 8). At day 28, the weight remaining ratio of *AC1* and *AC6* hydrogels was 65% and 78%, respectively.

Lastly, the higher stability of *AC6* gel is also evident from thermal analysis. Its higher T_g and T_m values provide further confirmation of its more compact nature. During hydrolysis, as for *AC1*, a decrease of T_g (from 245 to 242°C) can be detected, being probably due to the loss of esters bonds and consequently loss of network organization.[26]

CONCLUSIONS

Hydrolytic degradation of Agar-Carbomer based hydrogels was here studied, providing a better chemical understanding of all involved mechanisms and moieties, aiming at satisfying the growing request of finely controllable, biocompatible, and biodegradable polymeric systems for cell and drug delivery applications. Two sets of hydrogels, from the same material library, were investigated: their main compositional differences being related specifically to the amount of crosslinkers. Several works and reviews underlined how important it is for a scaffold to be nanostructured and consequently to mimic the natural environment to provide a better host response. Here, indeed, TEM observations confirmed the nanostructured nature of both gels and the effects of crosslinker on their intimate structure: their weighted presence produced a much tighter and tough matrix, in agreement with rheological and calorimetric data. FT-IR analysis provided a relevant insight on degradation that in both cases occurred via bulk hydrolysis, being water diffusion into gel matrix much faster than hydrolysis itself. Indeed, as degradation occurs, hydrolytically labile bonds are cleaved throughout the entire network. The speed of cleavage depends on the degree of crosslinking present in the matrix: by increasing it, degradation starts earlier due to higher concentration of hydrolyzable bonds but it lasts for a longer period due to the higher viscosity within the polymeric network. On the other hand, decreasing crosslinking density, degradation starts lately but it is less intense due to the lower compactness and viscosity of the network.

The present study underlines the role of polymers, crosslinkers, and their mutual ratio in hydrogel synthesis. It also provides an insight on how material properties are thereof affected, both during gelation and during degradation, in terms of time and magnitude, by chemically controlling the intimate 3D structure of the hydrogel. This information represents the required knowledge and the operative tool for the development and tuning of specific hydrogels as cell carriers and drug delivery systems for different specific tissue engineering applications, with the great practical advantage of sharing the same macromeric components.

References

1. Xu, Y.; Shi, Y.; Ding, S. Nature 2008, 453, 338.
2. Sakurada, K.; McDonald, F. M.; Shimada, F. Angew Chem Int Ed 2008, 47, 5718.
3. Wan, A. C. A.; Ying, J. Y. Adv Drug Deliv Rev 2010, 62, 731.
4. Huang, S.; Fu, X. B. J Control Release 2010, 142, 149.
5. Langer, R. Adv Mater 2009, 21, 3235.
6. Atala, R.; Langer, R.; Thomson, J; Nerem, R. Principles of Regenerative Medicine; Academic Press: Burlington, MA, 2008.
7. Mantsos, T.; Chatzistavrou, X.; Roether, J. A.; Hupa, L; Arstila, H.; Boccaccini, A. R. Biomed Mater 2009, 4, 055002.
8. Rezwan, K.; Chen, Q. Z.; Blaker, J. J.; Boccaccini, A. R. Biomaterials 2006, 27, 3413.
9. Hu, B. H.; Su, J.; Messersmith, P. B. Biomacromolecules 2009, 10, 2194.
10. Blaker, J. J.; Bismarck, A.; Boccaccini, A. R.; Young, A. M.; Nazhat, S. N. Acta Biomater 2010, 6, 756.
11. Nakamatsu, J.; Torres, F. G.; Troncoso, O. P.; Yuan, M. L.; Boccaccini, A. R. Biomacromolecules 2006, 7, 3345.
12. Slaughter, B. V.; Khurshid, S. S.; Fisher, O. Z.; Khademhosseini, A.; Peppas, N. A. Adv Mater 2009, 21, 3307.
13. Baumann, M. D.; Kang, C. E.; Tator, C. H.; Shoichet, M. S. Biomaterials 2010, 31, 7631.
14. Shoichet, M. S. Macromolecules 2010, 43, 581.
15. Brandl, F.; Kastner, F.; Gschwind, R. M.; Blunk, T.; Tessmar, J.; Gopferich, A. J Control Release 2010, 142, 221.
16. Hoare, T. R.; Kohane, D. S. Polymer 2008, 49 1993.
17. Tan, H. P.; Chu, C. R.; Payne, K. A.; Marra, K. G. Biomaterials 2009, 30, 2499.
18. Kim, Y. T.; Caldwell, J. M.; Bellamkonda, R. V. Biomaterials 2009, 30, 2582.
19. Jones, D. S.; Bruschi, M. L.; de Freitas, O.; Gremiao, M. P. D.; Lara, E. H. G.; Andrews, G. P. Int J Pharm 2009, 372, 49.
20. Rossi, F.; Perale, G.; Masi, M. Chem Pap 2010, 64, 573.
21. Tunesi, M.; Rossi, F.; Daniele, F.; Bossio, C.; Perale, G.; Bianco, F.; Matteoli, M.; Giordano, C.; Cigada, A. Regen Med 2009, 4, S295.
22. Santoro, M.; Marchetti, P.; Rossi, F.; Perale, G.; Castiglione, F.; Mele, A.; Masi, M. J Phys Chem B 2011, 115, 2503
23. Perale, G.; Veglianese, P.; Rossi, F.; Peviani, M.; Santoro, M.; Llupi, D.; Micotti, E.; Forloni, G.; Masi, M. Mater Lett 2011, 65, 1688
24. Gao, C. M.; Liu, M. Z.; Chen, J.; Zhang, X. Polymer Degrad Stabil 2009, 94, 1405.
25. Yan, H.; Saiani, A.; Gough, J. E.; Miller, A. F. Biomacromolecules 2006, 7, 2776.
26. Vidovic, E.; Klee, D.; Hocker, H. J Appl Polymer Sci 2009, 112, 1538.
27. Zhu, X. F.; Lu, P.; Chen, W.; Dong, J. A. Polymer 2010, 51, 3054.
28. Flory, P. J. Principles of Polymer Chemistry; Cornell Univeristy Press: New York, 1953.
29. van de Manakker, F.; Vermonden, T.; el Morabit, N.; van Nostrum, C. F.; Hennink, W. E. Langmuir 2008, 24, 12559.
30. Brandrup, J. Polymer Handbook, 4th ed.; Wiley, 2003.

31. Huglin, M. B.; Rehab, M. M. A. M.; Zakaria, M. B. Macromolecules 1986, 19, 2986.
32. de Jong, S. J; van Eerdenbrugh, B.; van Nostrum, C. F.; Kettenes-van de Bosch, J. J.; Hennink, W. E. J Control Release 2001, 71, 261.
33. Wang, J. J.; Li, X. S. J Appl Polymer Sci 2010, 116, 2749.
34. Estroff, L. A.; Leiserowitz, L.; Addadi, L.; Weiner, S.; Hamilton, A. D. Adv Mater 2003, 15, 38.
35. Nykaenen, A.; Nuopponen, M.; Hiekkataipale, P.; Hirvonen, S. P.; Soininen, A.; Tenhu, H.; Ikkala, O.; Mezzenga, R.; Ruokolainen, J. Macromolecules 2008, 41, 3243.
36. Karadag, E.; Kiristi, T.; Kundakci, S.; Uzum, O. B. J Appl Polymer Sci 2010, 117, 1787.
37. Peppas, N. A. Hydrogels in Medicine and Pharmacy; CRC Press: Boca Raton, FL, 1987.
38. Engel, E.; Michiardi, A.; Navarro, M.; Lacroix, D.; Planell, J. A. Trends Biotechnol 2008, 26, 39.
39. Flemming, R. G.; Murphy, C. J.; Abrams, G. A.; Goodman, S. L.; Nealey, P. F. Biomaterials 1999, 20, 573.
40. Dubinsky, S.; Grader, G. S.; Shter, G. E.; Silverstein, M. S. Polymer Degrad Stabil 2004, 86, 171.
41. Moharram, M. A.; Khafagi, M. G. J Appl Polymer Sci 2006, 102, 4049.
42. Zong, X.; Ran, S.; Kim, K. S.; Fang, D.; Hsiao, B. S.; Chu, B. Biomacromolecules 2003, 4, 416.
43. Jabr-Milane, L. S.; van Vlerken, L. E.; Yadav, S.; Amiji, M. M. Cancer Treat Rev 2008, 34, 592.